ANESTHESIOLOGY

Neurophysiologic Complexity in Children Increases with Developmental Age and Is Reduced by General Anesthesia

Michael P. Puglia II, M.D., Ph.D., Duan Li, Ph.D., Aleda M. Leis, M.S., Elizabeth S. Jewell, M.S., Chelsea M. Kaplan, Ph.D., Megan Therrian, B.S., Minkyung Kim, Ph.D., UnCheol Lee, Ph.D., George A. Mashour, M.D., Ph.D., Phillip E. Vlisides, M.D.

ANESTHESIOLOGY 2021; 135:813–28

EDITOR'S PERSPECTIVE

What We Already Know about This Topic

- Cortical complexity refers to the differentiation or diversity of neural activity patterns in the cerebral cortex
- In adults, changes in cortical complexity have been shown to reflect changes in the level of consciousness across different classes of general anesthetics
- Changes in cortical complexity with age and during general anesthesia in pediatric populations are incompletely understood

What This Article Tells Us That Is New

- Using the Lempel–Ziv algorithm, a mathematical method for assessing neural signal complexity, a positive correlation of cortical complexity with age was found in awake, 8- to 16-yr-old children
- During anesthetic state transitions in this pediatric population, cortical complexity decreased during the maintenance phase and, upon recovery of consciousness, remained reduced when compared with preanesthesia baseline levels

ABSTRACT

Background: Neurophysiologic complexity in the cortex has been shown to reflect changes in the level of consciousness in adults but remains incompletely understood in the developing brain. This study aimed to address changes in cortical complexity related to age and anesthetic state transitions. This study tested the hypotheses that cortical complexity would (1) increase with developmental age and (2) decrease during general anesthesia.

Methods: This was a single-center, prospective, cross-sectional study of healthy (American Society of Anesthesiologists physical status I or II) children (n = 50) of age 8 to 16 undergoing surgery with general anesthesia at Michigan Medicine. This age range was chosen because it reflects a period of substantial brain network maturation. Whole scalp (16-channel), wireless electroencephalographic data were collected from the preoperative period through the recovery of consciousness. Cortical complexity was measured using the Lempel–Ziv algorithm and analyzed during the baseline, premedication, maintenance of general anesthesia, and clinical recovery periods. The effect of spectral power on Lempel–Ziv complexity was analyzed by comparing the original complexity value with those of surrogate time series generated through phase randomization that preserves power spectrum.

Results: Baseline spatiotemporal Lempel–Ziv complexity increased with age (yr; slope [95% CI], 0.010 [0.004, 0.016]; $P < 0.001$); when normalized to account for spectral power, there was no significant age effect on cortical complexity (0.001 [–0.004, 0.005]; $P = 0.737$). General anesthesia was associated with a significant decrease in spatiotemporal complexity (median [25th, 75th]; baseline, 0.660 [0.620, 0.690] *vs.* maintenance, 0.459 [0.402, 0.527]; $P < 0.001$), and spatiotemporal complexity exceeded baseline levels during postoperative recovery (0.704 [0.642, 0.745]; $P = 0.009$). When normalized, there was a similar reduction in complexity during general anesthesia (baseline, 0.913 [0.887, 0.923] *vs.* maintenance 0.851 [0.823, 0.877]; $P < 0.001$), but complexity remained significantly reduced during recovery (0.873 [0.840, 0.902], $P < 0.001$).

Conclusions: Cortical complexity increased with developmental age and decreased during general anesthesia. This association remained significant when controlling for spectral changes during anesthetic-induced perturbations in consciousness but not with developmental age.

(ANESTHESIOLOGY 2021; 135:813–28)

Although the brain is a major target organ of general anesthetics, there remains no standard neurophysiologic monitor in the perioperative period. The lack of a standardized monitoring strategy likely reflects an incomplete understanding of the precise neural correlates of consciousness. Identifying neurobiological processes underlying consciousness is particularly challenging in the pediatric population, because the brain undergoes considerable structural and functional changes during development, resulting in substantial brain network formation and refinement.[1,2] Cortical oscillatory patterns and

This article is featured in "This Month in Anesthesiology," page A1. Supplemental Digital Content is available for this article. Direct URL citations appear in the printed text and are available in both the HTML and PDF versions of this article. Links to the digital files are provided in the HTML text of this article on the Journal's Web site (www.anesthesiology.org). This article has a visual abstract available in the online version.

Submitted for publication February 1, 2021. Accepted for publication July 14, 2021. Published online first on September 7, 2021. From the Department of Anesthesiology (M.P.P., D.L., A.M.L., E.S.J., C.M.K., M.T., M.K., U.L., G.A.M., P.E.V.), the Center for Consciousness Science (M.P.P., D.L., M.K., U.L., G.A.M., P.E.V.), and the Neuroscience Graduate Program (G.A.M.), University of Michigan Medical School, Ann Arbor, Michigan.

<zdoi;. DOI: 10.1097/ALN.0000000000003929>

spectral properties can thus vary considerably with age[3,4] and during general anesthesia.[5–8] In addition, network hubs (highly connected brain regions that facilitate information transfer) undergo significant developmental maturation[9–11] and are highly susceptible to functional disruption with general anesthesia.[12] As such, identifying age-invariant markers of anesthetic-induced unconsciousness is difficult for pediatric patients.

Candidate strategies for perioperative brain monitoring in the pediatric population need to account for neurodevelopmental changes that occur with age. One such strategy is the measure of neurophysiologic complexity in the cortex, hereafter referred to as cortical complexity. Cortical complexity can be broadly thought of as representing the differentiation or diversity of neural activity and can be analyzed using mathematical algorithms.[13–22] The Lempel–Ziv algorithm serves as one such method for assessing neural signal complexity. It is a method of symbolic sequence analysis used to measure the "compressibility" or variability of a data series. In adults, previous studies have demonstrated a correlation between changes in Lempel–Ziv complexity with changes in the level of consciousness across different classes of anesthetic agents.[14,15,21,23] However, cortical complexity has not been rigorously studied in pediatric populations requiring surgery and anesthesia. Analyzing Lempel–Ziv complexity thus serves as a candidate strategy for identifying changes in cortical signal complexity across various ages of neurodevelopment and during anesthetic-mediated perturbations in states of consciousness.

The objectives of this empirical and theoretical study were to determine the changes in cortical complexity with age and during general anesthesia. Specifically, this study tested the hypothesis that cortical complexity would increase with developmental age and decrease during general anesthesia. We studied a population of children 8 to 16 yr old because this age range reflects a period of dramatic brain network maturation. Additionally, children of this age are more likely to participate in preanesthetic assessment of baseline consciousness.

Materials and Methods

This was a prospective, single-center, cross-sectional, observational study assessing cortical complexity in children undergoing general anesthesia for elective outpatient surgery. The study was approved by the University of Michigan Medical School Institutional Review Board (Ann Arbor, Michigan; approval No. HUM00142298). After careful discussion, written informed consent by parents/guardians and verbal or written assent by pediatric patients were obtained before study enrollment. All study operations were conducted at C.S. Mott Children's Hospital, Michigan Medicine, University of Michigan. Recruitment took place from November 2018 to March 2020. This study adheres to the Strengthening the Reporting of Observational Studies in Epidemiology (STROBE) guidelines.[24] Statistical analysis plans for the primary and secondary outcomes and meaningful effect size were defined *a priori*.

Study Population

Pediatric patients aged 8 to 16 yr old, with American Society of Anesthesiologists physical status I or II, and scheduled for outpatient elective surgery with a halogenated ether as the primary anesthetic were eligible for study enrollment. Exclusion criteria included a patient history of seizure disorder, developmental delay, neurologic disease, current use of stimulant medications (*e.g.*, amphetamine, dextroamphetamine), surgery above the neck (which might preclude neurophysiologic monitoring), history or suspicion of a difficult airway, physical characteristics that prevent electrode contact with scalp, enrollment in conflicting research protocol, or where English was not the primary language.

Anesthetic and Perioperative Management

The goal of this study was to determine the changes in cortical complexity across age in the preoperative, baseline state of consciousness and through the perioperative period. As such, no protocol was implemented for altering patient care. Clinical teams provided care as indicated, based on standard perioperative protocols, and were blinded to the electroencephalogram data to prevent additional sources of bias.

Electroencephalographic Data Acquisition

The electroencephalogram was recorded from 16 Ag/AgCl scalp electrodes using a wireless electroencephalographic system (mobile 128 system, Cognionics Inc., USA) and applied based on the international 10-20 system (Supplemental Digital Content, fig. 1, http://links.lww.com/ALN/C668). Head circumference was measured to ensure proper cap size (EASYCAP, Germany). Cap placement was based on electrode position Cz, which was localized to half of the distance between the nasion and inion and the preauricular notch measurements. Data recordings were sampled at 500 samples/s and referenced to the mastoid. Electrode impedances were continuously monitored and maintained at less than 100 kΩ per manufacturer recommendations. The raw electroencephalogram signals were exported into MATLAB (version 2019b; MathWorks, Inc., USA) and downsampled to 250 Hz. The 60-Hz power-line interference, if present, was removed using a multitaper regression technique and Thomas F-statistics implemented in CleanLine plugin for EEGLAB toolbox.[25]

Epoch Selection and Preprocessing

Electroencephalogram epochs selected for data analysis are shown in figure 1. Baseline (n = 50) electroencephalogram data (range, 3.27 to 5.97 min) were recorded in the preoperative eyes-closed resting state. Premedication electroencephalogram data for all subjects were extracted from a 2-min segment that was recorded within 5 min before and

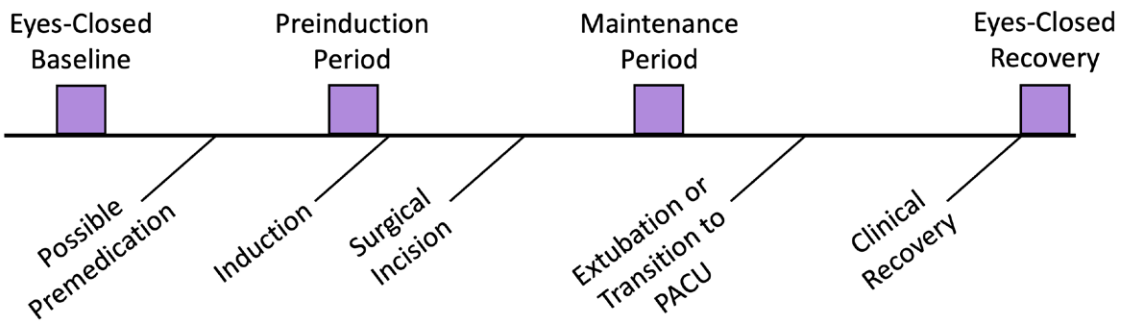

Fig. 1. Study paradigm. *Purple squares* represent epochs of electroencephalogram data that were extracted for analysis. PACU, postanesthesia care unit.

as close as possible to the induction of general anesthesia. If premedication was administered, the selected segment was at least 2 min after intravenous administration (n = 18) or 20 min after oral administration (n = 3). Maintenance (n = 49) electroencephalogram data (5 min) were recorded during the maintenance of general anesthesia and approximately halfway between surgical incision and cessation of the anesthetic maintenance agent. The specific time epoch chosen was based on the following additional criteria: constant age-adjusted minimum alveolar concentration value (greater than 0.7 and less than ±0.1% change) and electroencephalogram data suitable for analysis (*i.e.*, free from artifact by visual inspection). During this maintenance period, the mean age-adjusted minimum alveolar concentration value was 1.26 ± 0.35. Recovery (n = 45) electroencephalogram data (range, 1.18 to 5.75 min) were recorded in a postoperative, eyes-closed resting state after clinical recovery determined by achieving a University of Michigan Sedation Scale score of 0 to 1.[26] For the maintenance phase, one patient was excluded because of a minimum alveolar concentration below selection criteria, and five patients in the recovery phase were excluded because of data loss (*e.g.*, associated with emergence delirium).

For each epoch, the electroencephalogram signals were preprocessed as previously described.[27] First, bad channels and noisy time segments with obvious artifacts were rejected by visual inspection; the data after artifact removal had an average length (mean ± SD) of 4.88 ± 0.39 min with 15 to 16 channels for the baseline, 5 ± 0 min with 14 to 16 channels for the maintenance, and 3.06 ± 1.21 min with 11 to 16 channels for the recovery epochs. Second, the signals were detrended using a local linear regression method with a 10-s window at a 5-s step size in the Chronux analysis toolbox,[28] and low-pass-filtered at 50 Hz using the eegfiltnew function in the EEGLAB toolbox.[25] Third, the signals underwent independent component analysis using the extended-Infomax algorithm in the EEGLAB toolbox.[25] Independent components representing cardiac, eye, muscle, or other transient artifacts were identified and removed using visual inspection of the time-domain waveform, power spectrum, and spatial scalp topography. The number of independent components removed were (median [25th, 75th]) 3 [2, 4] for the baseline epochs, 0 [0, 0] for the maintenance epochs, and 4 [2, 5] for the recovery epochs.

Spectral Power

The power spectrogram was estimated using the multitaper method in the Chronux analysis toolbox,[28] with a window length of 4 s with 50% overlap, a time-bandwidth product of 2, and a number of tapers of 3; the estimates were then averaged over all available windows to obtain the averaged power spectrum for each available channel. The normalized power spectrum was further calculated as the absolute power spectrum divided by the total power at 0 to 50 Hz. Electroencephalogram power was calculated for delta (0.5 to 4 Hz), theta (4 to 7 Hz), alpha (7 to 13 Hz), beta (13 to 25 Hz), and gamma (25 to 50 Hz) from both absolute and normalized power spectra. The topographic maps of group-level spectral power across all subjects were constructed for each frequency band using the topoplot function in the EEGLAB toolbox.[25]

Complexity Analysis

We used the Lempel–Ziv algorithm to determine the complexity of cortical dynamics across different states. Lempel–Ziv complexity is a method of symbolic sequence analysis[18] that serves as a surrogate measure of temporal and spatiotemporal complexity of brain activity.[14–16,21,23] In this study, we assessed both spatiotemporal complexity across multiple channels and temporal complexity in individual channels.

The spatiotemporal complexity was measured as previously described.[23] Specifically, the instantaneous amplitude was estimated by applying the Hilbert transform, which was then segmented into 4-s windows with 50% overlap (additional analysis was performed to test the effect of window length; Supplemental Digital Content, fig. 2, http://links.lww.com/ALN/C668). The data were then converted to a

binary value using the mean value as the threshold for each channel. The data window was then converted into a binary matrix in which rows represent channels and columns represent time points. The complexity of the matrix was assessed by spatiotemporal Lempel–Ziv algorithm, which reflects the number of different spatial patterns across time. If the matrix is random, the spatiotemporal Lempel–Ziv complexity tends to be high; if channels behave similarly (or identically), Lempel–Ziv complexity is low. Because the Lempel–Ziv complexity value for a sequence of fixed length is maximal if it is entirely random, we normalized the raw spatiotemporal Lempel–Ziv complexity by the mean of those from n = 50 surrogate data generated by randomly shuffling the original spatial order for each time point; thus, the resultant spatiotemporal Lempel–Ziv complexity values range from 0 to 1. To test whether the Lempel–Ziv complexity is accounted for by spectral changes, we normalized the spatiotemporal Lempel–Ziv complexity by the mean of those from a surrogate time series (n = 50) generated through phase randomization that preserves the spectral profiles of the signal for each channel. If the complexity change is entirely due to spectral changes, the difference in the Lempel–Ziv complexity values across the states will be completely preserved in the Lempel–Ziv complexity values from the surrogate data; thus, the normalized spatiotemporal Lempel–Ziv complexity will be close to 1 and equal across the states. If the change in complexity is not due to spectral changes, the alterations of Lempel–Ziv complexity values from the surrogate data will be distinct from those of spatiotemporal Lempel–Ziv complexity, and the normalized spatiotemporal Lempel–Ziv complexity will reflect the signal diversity beyond the spectral changes. Last, the spatiotemporal Lempel–Ziv complexity and normalized spatiotemporal Lempel–Ziv complexity values were averaged across all available windows as the final estimate for each state and participant.

To measure individual-channel temporal complexity, the number of different temporal patterns in each individual channel was analyzed. These data were then normalized by the mean of those from n = 50 surrogate data generated by randomly shuffling the temporal order for each channel to obtain temporal Lempel–Ziv complexity. We further tested whether the difference in the Lempel–Ziv complexity across states is due to spectral changes by comparing the temporal Lempel–Ziv complexity with the mean of those from n = 50 surrogate time series generated through phase randomization. The temporal Lempel–Ziv complexity and normalized temporal Lempel–Ziv complexity values were averaged across all available windows as the final estimate for each channel, state, and participant. The topographic maps of group-level temporal complexity across all subjects were constructed using the topoplot function in the EEGLAB toolbox.[25] For each epoch and subject, the mean temporal complexity was further obtained by averaging the temporal Lempel–Ziv complexity (and normalized temporal Lempel–Ziv complexity) in prefrontal (Fp1, Fp2), frontal (F5, F6, Fz), central (C3, C4, Cz), parietal (P5, P6, Pz), and occipital (O1, O2) regions, as well as all further channels across the scalp.

Human Brain Network Simulations of Maturation

To assess the general relationship between brain network maturation and complexity, a large-scale functional brain network was simulated using a coupled Stuart–Landau model implemented in a neuroanatomically informed scaffolding derived from human diffusion tensor imaging. Complexity values of oscillations in the simulated brain network models were compared to assess the effect of developmental changes in the network hub structure. We chose the Stuart–Landau model because it can replicate the oscillatory dynamics of different types of brain signals.[29–32] The coupled Stuart–Landau model is defined as follows:

$$\dot{z}_j(t) = \left\{\lambda_j + i\omega_j - \left|z_j(t)\right|^2\right\} z_j(t) + \sum_{k=1}^{N} A_{jk} K_{jk} z_k\left(t - \tau_{jk}\right) + \beta\xi_j(t) \quad (1)$$

Here, the complex variable $z_j(t)$ determined a state of the node (brain region) j at time t, $j = 1, 2, \ldots, N$. The anatomical structure A was acquired from group-averaged diffusion tensor imaging with n = 82 nodes.[33] The A_{jk} is determined by the connection weight between brain regions j and k. We modulated A_{jk} to simulate brain network maturation based on previous studies demonstrating that hub structure is associated with the developmental age.[9–11,34] Therefore, we additionally used weak (one tenth lower in connection strength compared with the ten strongest hubs) and strong (five times larger in connection strengths compared with the ten strongest hubs) hub structures to simulate the effect of brain network maturation. The brain network model simulation described below was performed with three different brain anatomical structures. The dynamics of the oscillator settle on a limit cycle if $\lambda_j > 0$ and on a stable focus if $\lambda_j < 0$. We modulated the $\lambda_j = \lambda$ from −3 to 3 with $\delta\lambda = 0.2$. The ω_j is an initial angular natural frequency of each oscillator j. To simplify the model, we used a Gaussian distribution for natural frequency with a mean frequency of 10 Hz and SD of 0.3 Hz to simulate the narrow bandwidth of human electroencephalogram activity in the eyes-closed resting state.[30–32,35] We controlled a coupling term $K_{jk} = K$ between oscillators j and k from 0 to 0.5 with $\delta K = 0.01$, which determines the global connection strength among brain regions. To make the model more realistic, we introduced a time delay between brain regions, $\tau_{jk} = D_{jk} / s$, with the average speed of axons in brain areas, $s = 7$ ms[36] and the distance D_{jk} between brain regions. The brain region j receives input from connected region k after the time delay τ_{jk}. The model results are not qualitatively different if the time delay is smaller than a quarter of the period of oscillation.[31] A Gaussian white noise $\xi_j(t)$ for each region was added with the SD $\beta = 0.005$. We numerically solved the

differential equations of the Stuart–Landau model using the Stratonovich–Heun method with 1,000 discretization steps. The first 10 s of the generated signals were discarded, and the last 50 s were used for the analysis of each simulation. Each brain region generates its own spontaneous oscillatory dynamics in a network at each bifurcation parameter λ and coupling strength K for one simulation. The simulation was repeated 50 times with different frequency configurations to obtain statistical robustness.

Among the simulated brain signals at various bifurcation parameter λ and coupling strength K, we selected brain states at certain parameter sets that can represent conscious states. A variance of the level of global synchronization in a network, termed the pair correlation function, was calculated, and the state at certain coupling strength K with the largest pair correlation function was chosen as the state that can represent the conscious state for each bifurcation parameter λ.[32] The instantaneous global synchronization level $r(t)$ at time t was calculated using phase difference $\Delta\theta_{jk}(t) = \theta_j(t) - \theta_k(t)$ at each coupling strength K.

$$r(t) = \left\langle \left| \frac{1}{N} \sum_{k=1}^{N} e^{i\Delta\theta_{jk}(t)} \right| \right\rangle \quad (2)$$

Here $r(t) = 1$ if all phases are equal, but $r(t)$ is nearly 0 if all phases are randomly distributed.

Global pulsatile stimuli to the whole brain network were induced at the states with the largest pair correlation function to observe the complexity from the response to the stimuli. The coupled Stuart–Landau model with the stimulation term $u(t)$ is as follows:

$$\dot{z}_j(t) = \left\{ \lambda_j + i\omega_j - |z_j(t)|^2 \right\} z_j(t) + \sum_{k=1}^{N} A_{jk} K_{jk} z_k(t - \tau_{jk}) + \beta \xi_j(t) + u(t) \quad (3)$$

$$u(t) = \begin{cases} p, & t_1 < t < t_2 \\ 0, & otherwise \end{cases} \quad (4)$$

Here p is the strength of the stimulus during a period $T = t_2 - t_1$. We fixed $p = 30$ and set duration of the stimulus as $T = 100$ ms. We induced the stimulus at 10 different random timings for one iteration. Each stimulus was applied independently to generated signals within one frequency configuration.

A significant response was calculated by comparing the instantaneous amplitude values $I(t)$ before and after the stimuli. For each iteration, the $I(t)$ of each node j after stimuli was normalized by the mean and SD of the baseline amplitude values of node j. Baseline values were obtained by using a total of 100 s, consisting of 10 trials of a 10-s prestimulus segment for each iteration. We considered the one tail $(1-\alpha)*100$th quantile with $\alpha = 0.05$ as a significantly increased amplitude. A perturbation response (represented in equations as PR) of node j at time t was defined in a binary fashion: $PR_j(t) = 1$, for the significantly increased amplitude for node j, and $PR_j(t) = 0$, otherwise. The complexity was calculated by measuring Lempel–Ziv complexity $LZc(t)$ of the $PR(t)$ over 1 s after the stimuli. The Lempel–Ziv complexity was calculated for brain network models with low, intermediate, and high hub structure connectivity.

Effect of Premedication on the Resting Electroencephalogram

To assess the effects of premedication on cortical complexity and spectral properties, the resting electroencephalogram data during the preinduction period were analyzed. The electroencephalogram signals were preprocessed as described for the primary analysis and, after preprocessing, 12 to 16 channels remained for n = 50 subjects. The spectral power and cortical complexity measures were calculated as described for the complexity analysis.

Statistical Analysis and Power Calculation

Statistical analyses were performed using MATLAB, and the data were tested for normality of distribution by Lilliefors corrected Kolmogorov–Smirnov tests. Because the null hypothesis of normality of distribution was rejected in some of the data sets ($P < 0.05$), the two-sided Wilcoxon signed rank test was used to compare the electroencephalogram measure (spectral power and cortical complexity) across baseline, maintenance, and recovery. With Bonferroni correction, $P < 0.017$ (0.05/3; 3 pairs) was considered statistically significant. Spearman correlation was used to investigate the relationship between age and each electroencephalogram measure. Univariate linear regressions, with age as the independent variable and complexity measures as the dependent exposure variables, were used to determine the slope [95% CI] of the associations, with R^2 used to assess goodness-of-fit. For the effect of premedication, the two-sided Wilcoxon rank sum test was used to compare the electroencephalogram measure (median [25th, 75th]) between subjects without (n = 29) and with premedication (n = 21). A Kruskal–Wallis test was used to calculate the statistical differences (median [25th, 75th]) across simulated brain networks, and $P < 0.05$ was considered statistically significant.

A sample size of 41 achieved 80% power to detect a change in slope between complexity and age from 0.000 under the null hypothesis to 0.011 under the alternative hypothesis when the statistical hypothesis is two-sided, the significance level is 0.050, the variance of age is 1.0816, the variance of complexity is 0.0009, the error variance of complexity is 0.5, and the correlation between observations within an individual is 0.25, assuming a compound symmetry correlation structure. This was a conservative estimate based on a previous study of complexity in healthy control patients of similar ages.[19]

Results

In total, 175 children were screened for study eligibility. Of the 175 who met the study criteria, 36 children declined participation, 52 were excluded because of operative time change or time constraints, 37 because of enrollment in another study, 21 because of research staff availability, 10 because of cancellation or no show for surgery, 3 because of changes in anesthetic plan, and 2 because of technical complications, leaving 50 participants who completed the study and were included for analysis. The participant demographic, anesthetic, and surgical characteristics are presented in table 1. Five participants had incomplete data for race.

Spectral Analysis

Age-related changes in spectral properties are shown in figure 2. Baseline normalized gamma power in the frontal and parietal region and beta in the parietal region were correlated with age (gamma: frontal $r = 0.30$, $P = 0.034$, and parietal $r = 0.31$, $P = 0.027$; beta: parietal $r = 0.40$, $P = 0.003$), whereas baseline theta was inversely correlated with age ($r = –0.45$, $P = 0.001$ and $r = –0.57$, $P < 0.001$ for frontal and parietal regions, respectively). Total power decreased with age, with a peak observed at 8 yr, and subsequent decreases were present during the baseline (slope [95% CI], –0.63 [–0.91, –0.35]; $P < 0.001$; $R^2 = 0.29$), maintenance (–0.65 [–0.94, –0.35]; $P < 0.001$; $R^2 = 0.28$), and recovery phases (–1.2 [–1.6, –0.79]; $P < 0.001$; $R^2 = 0.43$); Supplemental Digital Content, fig. 3, http://links.lww.com/ALN/C668). Total power also tended to decrease across regions and frequency bands with increasing age (Supplemental Digital Content, fig. 3, http://links.lww.com/ALN/C668). During maintenance, there was an inverse correlation for normalized theta power in the parietal region ($r = –0.32$, $P = 0.027$). During recovery, there was an inverse correlation for normalized delta power $r = –0.44$, $P = 0.002$ and $r = –0.35$, $P = 0.020$ for frontal and parietal regions, respectively). Conversely, higher (beta and gamma) frequencies were positively correlated during recovery (beta: frontal $r = 0.45$, $P = 0.002$ and parietal $r = 0.57$, $P < 0.001$; gamma: frontal $r = 0.51$, $P < 0.001$ and parietal $r = 0.53$, $P < 0.001$; fig. 2, A and B).

Group-level changes in spectral properties are shown in figure 3 (and Supplemental Digital Content, fig. 4, http://links.lww.com/ALN/C668). Overall, during general anesthesia, there were global increases in delta power and alpha anteriorization and decreases in the higher frequency band power (beta and gamma; fig. 3, A and B). In terms of total power, general anesthesia induced an overall increase in power (except for gamma), which returned to baseline level after recovery for most frequencies (except alpha; Supplemental Digital Content, fig. 4, http://links.lww.com/ALN/C668).

Table 1. Participant Characteristics

Participant Characteristics (n = 50)	
Age, yr (mean ± SD)	13 ± 2.4
Age, no. (%)	
8 to 10	15 (30)
11 to 13	21 (42)
14 to 16	14 (28)
Female sex, no. (%)	21 (42)
Race, no. (%)	
White	41 (82)
Black or African American	4 (8)
Other/unknown	5 (10)
Anesthetic duration, min (mean ± SD)	85 ± 44.7
Surgical type, no. (%)	
Orthopedic	25 (50)
Urology	14 (28)
General	10 (20)
Gynecology	1 (2)
Age-adjusted minimum alveolar concentration (mean ± SD)	1.26 ± 0.35
Maintenance agent, no. (%)	
Sevoflurane	24 (48)
Sevoflurane + nitrous oxide	5 (10)
Isoflurane	15 (30)
Isoflurane + nitrous oxide	6 (12)

Age-related Changes in Cortical Complexity

In the preanesthetic baseline state of consciousness, there was a positive correlation with age and spatiotemporal Lempel–Ziv complexity ($r = 0.41$, $P = 0.003$), as well as age and averaged temporal Lempel–Ziv complexity ($r = 0.39$, $P = 0.005$). Likewise, there was a significant linear association with age for both measures (slope [95% CI], 0.010 [0.004, 0.016], $P < 0.001$, $R^2 = 0.20$; and 0.007 [0.003, 0.011], $P < 0.001$, $R^2 = 0.20$, respectively; fig. 4, A and B). When these data were normalized to account for spectral effects, there was no correlation for the normalized spatiotemporal Lempel–Ziv complexity or normalized averaged temporal Lempel–Ziv complexity ($r = 0.02$, $P = 0.916$ and $r = 0.08$, $P = 0.572$). Likewise, the linear association was not statistically significant (slope [95% CI], 0.001 [–0.004, 0.005], $P = 0.737$, $R^2 < 0.01$, and 0.002 [–0.001, 0.004], $P = 0.234$, $R^2 = 0.03$, respectively; fig. 4, C and D). Regional analysis of temporal Lempel–Ziv complexity and normalized temporal Lempel–Ziv complexity mirrored the findings above for the whole brain average (data not shown). The results were qualitatively similar when we applied robustness testing by varying the duration of window analysis (Supplemental Digital Content, fig. 2A, http://links.lww.com/ALN/C668).

Effect of Brain Network Maturation on Complexity in Simulated Human Brain Models

Because our study design presumed but did not measure brain network development in the cohort of participants, we employed a principled approach to assess complexity in developing networks, as defined by networks that had

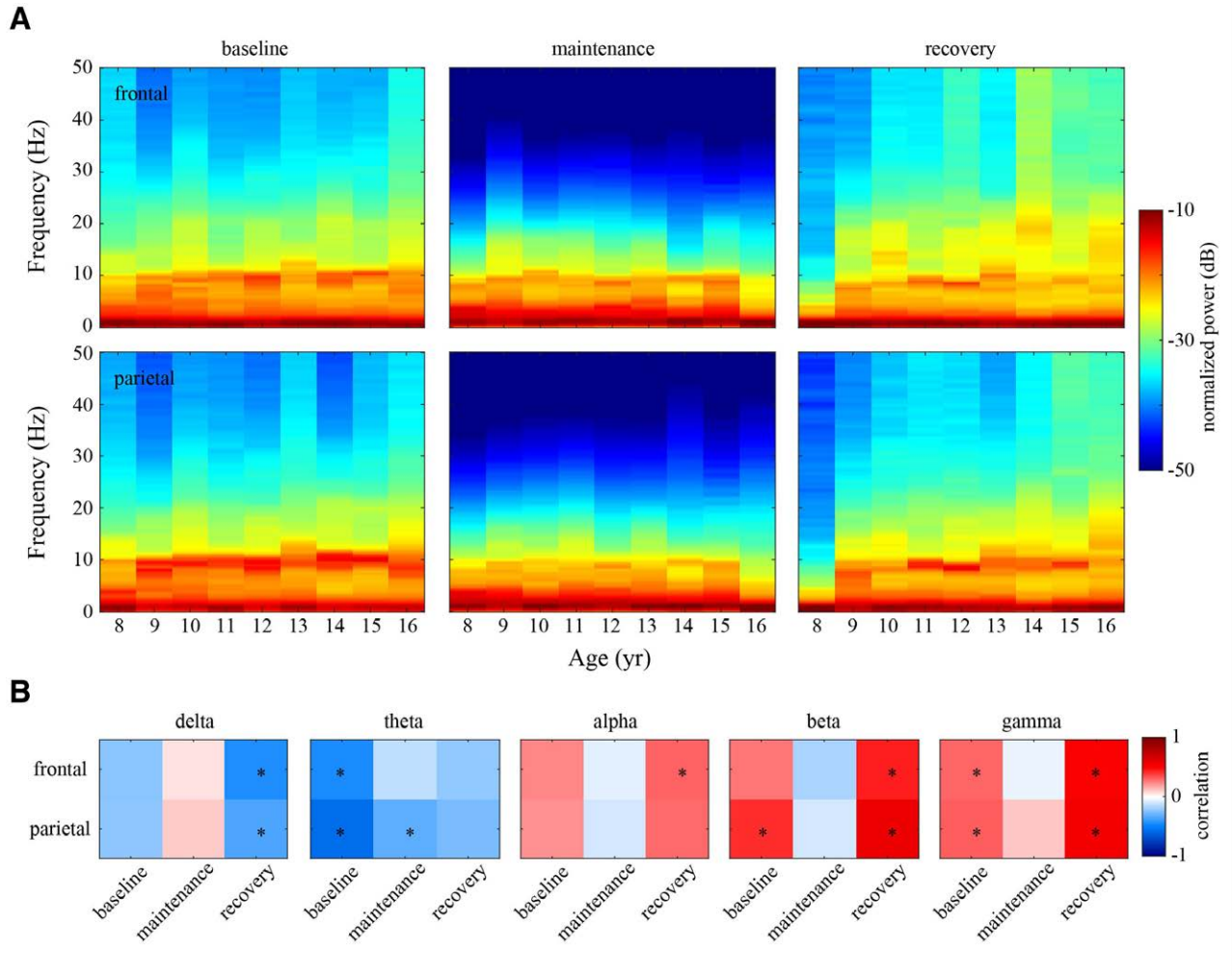

Fig. 2. Age-related changes in normalized spectral properties. (*A*) Group-level spectra of normalized electroencephalogram power as a function of age in the frontal (*top row*) and parietal (*bottom row*) brain regions across the baseline, maintenance, and recovery periods. (*B*) Spearman correlation between age and normalized electroencephalogram power in the frontal and parietal brain regions for each frequency band across the baseline, maintenance, and recovery periods. *Significant correlation with $P < 0.05$.

progressively increased hub structures. After a simulated perturbation, complexity was measured in computational brain models informed by human neuroanatomy and compared across weak, intermediate, and strong hub structures (as quantitatively defined under "Materials and Methods"). Lempel–Ziv complexity significantly increased across simulated brain models with increasing strength of connectivity in the network hub structure ($P < 0.001$; fig. 5).

Effect of Midazolam Premedication on Electroencephalogram Power and Cortical Complexity

Midazolam premedication was not associated with a change in cortical complexity when measured across the entire brain (fig. 6A). However, regional increases in complexity were found for both the temporal Lempel–Ziv complexity and normalized temporal Lempel–Ziv complexity in the central region (median [25th, 75th], 0.384 [0.352, 0.418] *vs.* 0.434 [0.414, 0.452], $P = 0.002$; 0.915 [0.898, 0.933] *vs.* 0.945 [0.915, 0.961], $P = 0.014$, respectively) and parietal region (0.377 [0.365, 0.401] *vs.* 0.420 [0.412, 0.456], $P < 0.001$; 0.923 [0.900, 0.939] *vs.* 0.938 [0.915, 0.958], $P = 0.031$, respectively; fig. 6, B and C). Midazolam premedication was associated with frequency- and region-specific changes in normalized electroencephalogram power (Supplemental Digital Content, fig. 5, http://links.lww.com/ALN/C668). In all brain regions, there was a decrease in theta and increase in beta power, as well as a decrease in frontal and prefrontal alpha power ($P < 0.05$).

Effects of General Anesthesia on Cortical Complexity

During the stable maintenance phase of general anesthesia, cortical complexity decreased from baseline values for both

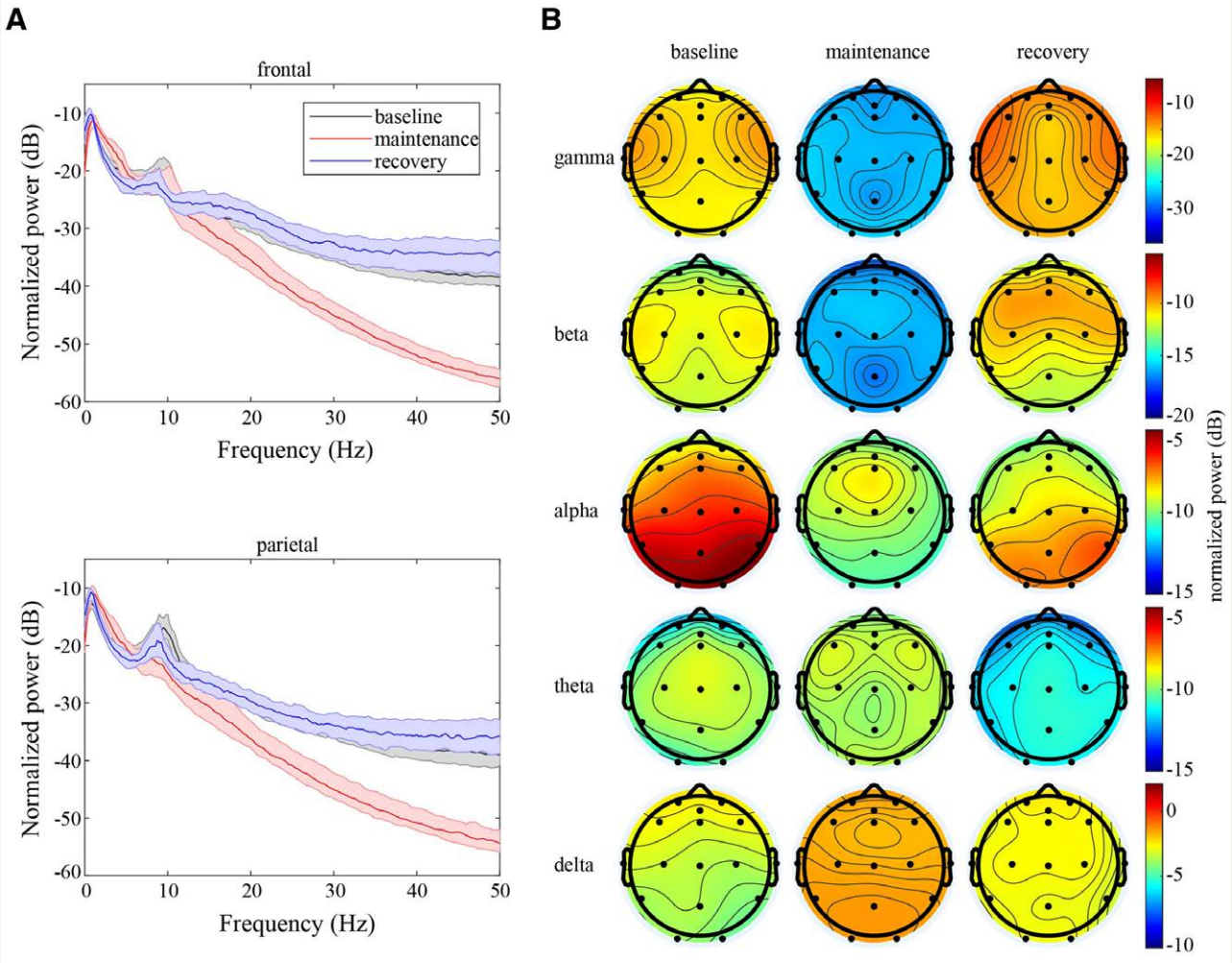

Fig. 3. Group-level spectral properties of normalized power. (*A*) Normalized power as a function of frequency for the baseline, maintenance, and recovery periods in the frontal (*top*) and parietal (*bottom*) brain regions. The *solid line* represents the median value, with *shading* representing the interquartile range. (*B*) Topographical representation of the normalized power for each frequency band for the baseline, maintenance, and recovery periods (note the differences in *scale bars* for each frequency band).

complexity measures tested, with the greatest decrease from baseline in spatiotemporal Lempel–Ziv complexity (median [25th, 75th] for baseline 0.660 [0.620, 0.690] *vs.* maintenance 0.459 [0.402, 0.527], $P < 0.001$; fig. 7; Supplemental Digital Content, fig. 6, http://links.lww.com/ALN/C668). Changes in complexity were independent of spectral power during the maintenance phase of general anesthesia. During recovery, spatiotemporal Lempel–Ziv complexity exceeded the baseline level (0.704 [0.642, 0.745], $P < 0.001$); however, after controlling for spectral changes, the normalized spatiotemporal Lempel–Ziv complexity during recovery was significantly decreased compared with baseline (baseline 0.913 [0.887, 0.923], *vs.* recovery 0.873 [0.840, 0.902], $P < 0.001$). Similar results were found for the average temporal Lempel–Ziv complexity analysis, with the exception of the normalized average temporal Lempel–Ziv complexity when the recovery period returned to baseline levels (0.960 [0.949, 0.966] *vs.* 0.957 [0.945, 0.965], $P = 0.404$, respectively). Regional changes in normalized temporal Lempel–Ziv complexity results were similar to data from the whole brain average (Supplemental Digital Content, fig. 7, http://links.lww.com/ALN/C668). Overall, these results were consistent when we varied the analysis window duration (Supplemental Digital Content, fig. 2B, http://links.lww.com/ALN/C668).

In a *post hoc* analysis of changes in spatiotemporal Lempel–Ziv complexity during the maintenance epoch with (n = 11) or without (n = 38) the use of nitrous oxide, there was no difference except that the normalized spatiotemporal Lempel–Ziv complexity was higher in the nitrous oxide group ($P = 0.045$, Wilcoxon rank sum test; data not shown). In an additional *post hoc* analysis of the

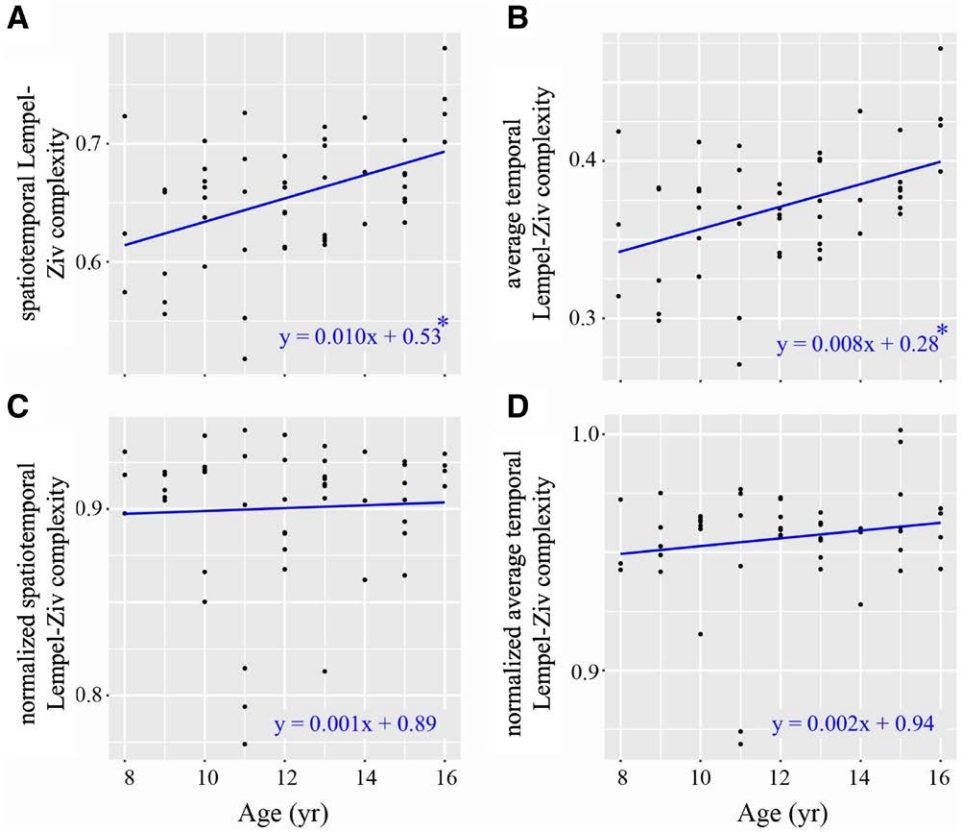

Fig. 4. Age-related changes in cortical complexity during the preanesthetic baseline. (*A*) Spatiotemporal Lempel–Ziv complexity. (*B*) Average temporal Lempel–Ziv complexity. (*C*) Normalized spatiotemporal Lempel–Ziv complexity. (*D*) Normalized average temporal Lempel–Ziv complexity of electroencephalogram data from the eyes-closed preanesthetic baseline period. The *blue line* represents the linear regression for each complexity measure with the line equation in the *bottom right* of each box. *Significant linear association ($P < 0.001$).

association of spatiotemporal Lempel–Ziv complexity and the average age-adjusted minimum alveolar concentration (maintenance epoch) with or without the use of nitrous oxide, we found a negative correlation (with nitrous oxide $r = -0.64$, $P = 0.040$, without $r = -0.36$, $P = 0.028$; Spearman correlation; data not shown), but this was not significant after controlling for spectral changes (with nitrous oxide $r = -0.37$, $P = 0.261$, without $r = -0.02$, $P = 0.916$; similar results were found for average temporal Lempel–Ziv complexity; data not shown).

Discussion

This study of children undergoing surgical anesthesia tested the hypothesis that electroencephalogram cortical complexity would increase with developmental age and decrease with general anesthesia. Age was positively correlated with cortical complexity during baseline recordings, and further analyses revealed that this was attributable to spectral changes. We supported this empirical finding through a principled approach by investigating complexity in simulated brain networks representative of development. This analysis demonstrated increased complexity with increasing connectivity strength of the network hub structure. During anesthetic state transitions, we found that cortical complexity decreased during the maintenance phase of general anesthesia compared with the eyes-closed baseline. Furthermore, after recovery of consciousness, normalized spatiotemporal complexity remained reduced compared with baseline. Overall, we found that age and anesthetic-mediated perturbations in the level of consciousness were associated with changes in cortical complexity, with age-related changes likely resulting from spectral changes and, as suggested by our simulation results, evolving functional architecture.

The hypothesis that cortical complexity would increase as a function of age was informed by the developmental maturation occurring through this period. Structural and functional changes, such as increased white matter density, long-range connections,[1,37] and network connectivity,[1,38] could yield a less reducible and more "complex" brain network. Additionally, studies of childhood and adolescent

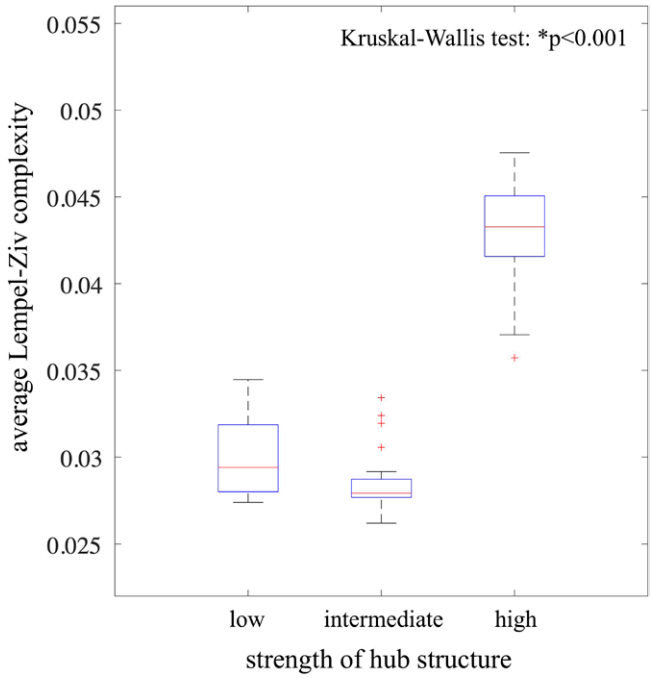

Fig. 5. Lempel–Ziv complexity of simulated brain models with changes in the connection strength of network hubs. The *central mark* in each box represents the median value, with the *edges* representing the 25th and 75th percentiles. The extending *whiskers* are the most extreme data points determined by the MATLAB algorithm (version 2019b; MathWorks, Inc., USA) to be nonoutliers, and the *red crosses* are those values deemed to be outliers. *Significance was measured using the Kruskal–Wallis test ($P < 0.001$).

brain network development have demonstrated increased differentiation, specialization, and organization of network function,[1,9,38] potentially leading to a greater diversity of neural oscillatory activity and measurable using complexity algorithms. Indeed, previous studies of resting state magnetoencephalogram data analyzed using the Lempel–Ziv complexity algorithm demonstrated a significant increase in complexity during childhood and adolescence that continued throughout the lifespan, peaking in the sixth decade.[19,20] Our results are consistent with this, but the effect is attributable to changes in spectral properties, which were not controlled for in the studies by Fernández *et al.*[19,20] The lack of an age effect in complexity beyond spectral properties is somewhat surprising given the magnitude of brain network change occurring during this period but is possibly accounted for by several factors. First, we did not control for developmental heterogeneity. It also remains possible that the normalized measure of complexity is not sensitive enough to measure a developmental difference but requires significantly larger perturbations (*e.g.*, anesthetic state transitions). The robust finding of significant decreases during general anesthesia, even when controlling for spectral changes, supports this interpretation. It should also be considered that despite the large developmental changes occurring in children 8 to 16 yr old, it remains possible that this age range may not capture the structural and functional changes required for discernable differences in normalized complexity. Additionally, a developing network may give rise to both spectral and complexity changes that temporally align.[39] Our computational brain model findings that networks with stronger hub structures yield a more complex network further support the empirical age-related results. Moreover, previous work from our group has shown that network hub structure is disrupted with propofol administration and consistent with reductions in complexity with general anesthesia.[12]

Complexity analysis using the Lempel–Ziv algorithm yielded dynamic results. Preoperative midazolam administration increased complexity in the central and parietal regions, whereas complexity was globally reduced during general anesthesia. Previous studies from our group demonstrated a similar increase in complexity with subanesthetic ketamine administration and reduction during ketamine anesthesia.[23] Although the mechanism for increased complexity during subanesthetic states remains unknown, it has been shown that γ-aminobutyric acid type A receptor agonists, such as propofol, can induce paradoxical excitation.[40] Additionally, benzodiazepines have been shown to increase beta activity in the central and parietal regions consistent with the increased beta activity we observed.[41,42] In support, a *post hoc* analysis

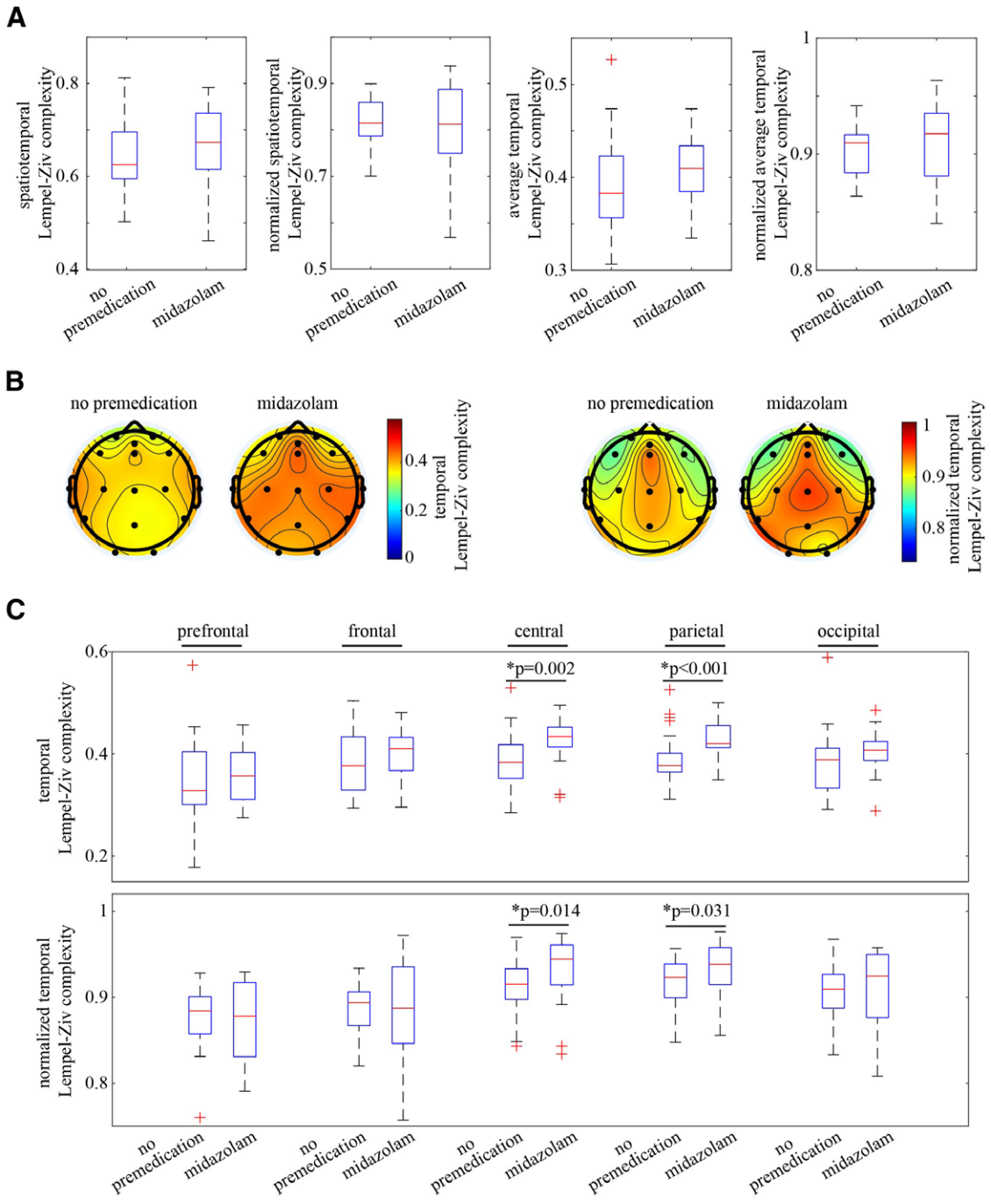

Fig. 6. Effect of premedication with midazolam on cortical complexity. (*A*) Spatiotemporal Lempel–Ziv complexity, normalized spatiotemporal Lempel–Ziv complexity, average temporal Lempel–Ziv complexity, and normalized average temporal Lempel–Ziv complexity of electroencephalogram data before the first intraoperative anesthetic medication administration. (*B*) Topographical representation of temporal Lempel–Ziv complexity and normalized temporal Lempel–Ziv complexity with and without midazolam premedication. (*C*) Region-wise analysis of the temporal Lempel–Ziv complexity and normalized temporal Lempel–Ziv complexity. For (*A*) and (*C*), the *central mark* in each box represents the median values, with the *edges* representing the 25th and 75th percentiles. The extending *whiskers* are the most extreme data points determined by the MATLAB algorithm (version 2019b; MathWorks, Inc., USA) to be nonoutliers, and the *red crosses* are those values deemed to be outliers. *Significance (*P* value shown); Wilcoxon rank sum test.

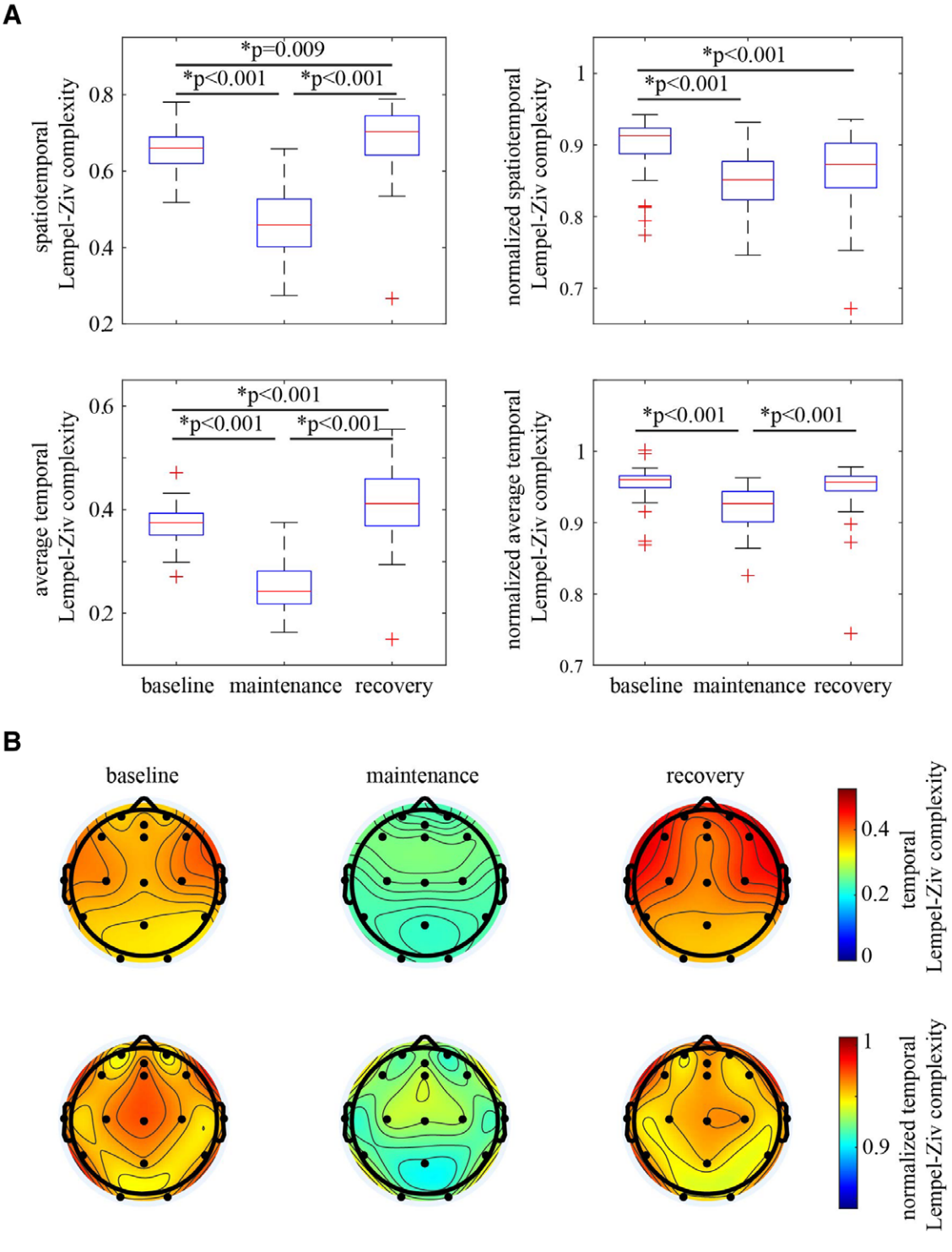

Fig. 7. Effect of general anesthesia on cortical complexity. (*A*) Spatiotemporal Lempel–Ziv complexity (*top left*), average temporal Lempel–Ziv complexity (*bottom left*), normalized spatiotemporal Lempel–Ziv complexity (*top right*), and normalized average temporal Lempel–Ziv complexity (*bottom right*) of electroencephalogram data for the baseline, maintenance, and recovery periods. (*B*) Topographical representation of the temporal Lempel–Ziv complexity and normalized temporal Lempel–Ziv complexity for the baseline, maintenance, and recovery periods. For (*A*), the *central mark* in each box represents the median value, with the *edges* being the 25th and 75th percentiles. The extending *whiskers* are the most extreme data points determined by the MATLAB algorithm (version 2019b; MathWorks, Inc., USA) to be nonoutliers, and the *red crosses* are those values deemed to be outliers. *Significance (*P* value shown); Wilcoxon signed rank test with Bonferroni correction for three pairwise comparisons.

of temporal complexity and beta power demonstrated a positive correlation and after controlling for spectral changes, was mitigated in the no-premedication group, but remained significant for the midazolam group (Supplemental Digital Content, fig. 8, http://links.lww.com/ALN/C668). This suggests an association between complexity and beta power, which could be a concurrent effect of midazolam on the electroencephalogram. However, a recent study of subanesthetic nitrous oxide administration demonstrated decreased electroencephalographic complexity (Shannon complexity).[13] The effect of various subanesthetic medications on cortical complexity in children remains an open question. In addition, there may be region specific changes (fig. 7B), but further investigation including high-density recordings would be required to address this fully.

Leading theories of consciousness posit that the diversity of information in both space and time is important for conscious processing.[43,44] The biologic interpretation of decreases in cortical complexity may represent reduced information sharing or processing. In this study, decreases in cortical complexity induced by general anesthesia were similar to what has been shown in animal models[16,45] and adult patients.[14,17,21,23] The significant decrease during general anesthesia of cortical complexity, independent of spectral changes, suggests that measures of complexity may be helpful in the development of real-time monitoring modalities across the adult and pediatric populations. It is important to note that complexity measures in this study reflect the level of consciousness despite the age-related changes in power occurring during this period of massive neurodevelopment. When developing monitoring systems, measures of the conscious state need to be robust, have high fidelity, and be accurate across the population. In our study, there was a decrease in all children with both spatiotemporal and averaged temporal complexity; however, when the data were normalized, nine children in the spatiotemporal and seven in the averaged temporal complexity analysis groups had actual increases in complexity during the maintenance of general anesthesia (Supplemental Digital Content, fig. 6, http://links.lww.com/ALN/C668). Additional *post hoc* analysis of age, anesthetic dose, or channel rejection did not account for this increase (data not shown). Recent work by our group in an animal model artificially dissociated the observed level of consciousness from various electroencephalographic measures, including complexity.[16] However, as noted in this study, just because state-related and neurophysiologic dynamic changes can be dissociated in the laboratory setting does not mean that they are not correlated during spontaneous physiologic, pharmacologic, or pathologic state transitions. These findings suggest that a single quantitative surrogate of consciousness using normalized complexity analysis may be insufficient to reliably determine the level of consciousness in all patients and future developmental studies should also address combinatorial surrogate measures. In addition, the finding of decreased normalized spatiotemporal complexity after clinical recovery is not surprising considering that functional brain network recovery extends beyond the initial return of consciousness.[46,47]

In an effort to confirm that our findings were consistent with the spectral characteristics across development shown in previous works, we analyzed both the absolute and normalized power of the electroencephalogram in this cohort. Similar to previous studies of school-age and adolescent children, we observed an age-dependent decrease in absolute electroencephalogram power over most brain regions during general anesthesia.[5,8] In addition, when the power data were normalized, regional differences were aligned with developmental structural and functional changes occurring during this period.[1,48] Specifically, there was a general shift toward faster oscillatory activity (*i.e.*, decreased theta and increased beta and gamma power).[3,4] When we analyzed the spectral data during general anesthesia, we found increased absolute power, increased delta power, decreased gamma power, and anteriorization of the alpha activity, consistent with what has been previously shown during this developmental period.[5,49,50]

Limitations

There are several limitations of this investigation. First, this was an observational study without a protocol for a standard anesthetic regimen, and although this was pragmatic, we are unable to dissect the role of individual anesthetic agents. We performed a *post hoc* analysis to investigate the role of nitrous oxide and minimum alveolar concentration values influence on complexity. Although we are cautious in interpreting these data because of the small subsamples, the findings were consistent with the overall findings. Additionally, patient characteristics that may be present and attributable to heightened preoperative anxiety could also influence complexity and spectral properties. Further, sex differences have been shown to affect cortical complexity with development, and future larger-scale studies should address this.[20] When considering the Lempel–Ziv complexity measure, there are several notable strengths: it is a nonparametric measure, can be applied to relatively short data segments, and can be used with nonstationary data. However, because the measure requires binarization of the original signal, there exists the possibility for the loss of information during the analysis as well as influence by slow waves in the electroencephalogram (Supplemental Digital Content, fig. 9, http://links.lww.com/ALN/C668). Additionally, this study was conducted in the perioperative environment and limited by a low electroencephalogram (16 channel) density and, in some instances, a loss of information from an electroencephalogram channel that has the potential to influence the assessment of cortically complexity. However, when we repeated our analysis excluding participants with channel rejection, the results were similar (data not shown).

In summary, cortical complexity increased with developmental age and decreased during general anesthesia. The age-related increase in cortical complexity could be

accounted for by spectral properties but, based on modeling data, is consistent with a maturing brain network. By contrast, reductions in complexity during general anesthesia extended beyond spectral properties. Overall, these findings contribute to the growing body of literature on cortical complexity and how this potential neural correlate of consciousness is affected by age and anesthetic state transitions.

Acknowledgments

The authors thank the children and their families for their participation in this study.

Research Support

Supported by Foundation for Anesthesia Education and Research (Schaumburg, Illinois) grant No. 20-PAF00823 and by the Department of Anesthesiology, University of Michigan Medical School, Ann Arbor, Michigan.

Competing Interests

Dr. Kaplan has received research funding from Lundbeck Biopharmaceutical Company (Copenhagen, Denmark). The other authors declare no competing interests.

Correspondence

Address correspondence to Dr. Puglia: 4-911 Mott Hospital, University of Michigan, 1540 E. Hospital Dr., SPC 4245, Ann Arbor, Michigan 48109-4245. mpuglia@med.umich.edu.

References

1. Menon V: Developmental pathways to functional brain networks: Emerging principles. Trends Cogn Sci 2013; 17:627–40
2. Gogtay N, Giedd JN, Lusk L, Hayashi KM, Greenstein D, Vaituzis AC, Nugent TF III, Herman DH, Clasen LS, Toga AW, Rapoport JL, Thompson PM: Dynamic mapping of human cortical development during childhood through early adulthood. Proc Natl Acad Sci USA 2004; 101:8174–9
3. Clarke AR, Barry RJ, McCarthy R, Selikowitz M: Age and sex effects in the EEG: Development of the normal child. Clin Neurophysiol 2001; 112:806–14
4. Gasser T, Verleger R, Bächer P, Sroka L: Development of the EEG of school-age children and adolescents: I. Analysis of band power. Electroencephalogr Clin Neurophysiol 1988; 69:91–9
5. Akeju O, Pavone KJ, Thum JA, Firth PG, Westover MB, Puglia M, Shank ES, Brown EN, Purdon PL: Age-dependency of sevoflurane-induced electroencephalogram dynamics in children. Br J Anaesth 2015; 115:i66–76
6. Cornelissen L, Donado C, Lee JM, Liang NE, Mills I, Tou A, Bilge A, Berde CB: Clinical signs and electroencephalographic patterns of emergence from sevoflurane anaesthesia in children: An observational study. Eur J Anaesthesiol 2018; 35:49–59
7. Pappas I, Cornelissen L, Menon DK, Berde CB, Stamatakis EA: δ-Oscillation correlates of anesthesia-induced unconsciousness in large-scale brain networks of human infants. Anesthesiology 2019; 131:1239–53
8. Koch S, Stegherr AM, Mörgeli R, Kramer S, Toubekis E, Lichtner G, von Dincklage F, Spies C: Electroencephalogram dynamics in children during different levels of anaesthetic depth. Clin Neurophysiol 2017; 128:2014–21
9. Oldham S, Fornito A: The development of brain network hubs. Dev Cogn Neurosci 2019; 36:100607
10. Cao M, Huang H, Peng Y, Dong Q, He Y: Toward developmental connectomics of the human brain. Front Neuroanat 2016; 10:25
11. Grayson DS, Ray S, Carpenter S, Iyer S, Dias TG, Stevens C, Nigg JT, Fair DA: Structural and functional rich club organization of the brain in children and adults. PLoS One 2014; 9:e88297
12. Lee H, Mashour GA, Noh GJ, Kim S, Lee U: Reconfiguration of network hub structure after propofol-induced unconsciousness. Anesthesiology 2013; 119:1347–59
13. Vrijdag XCE, van Waart H, Mitchell SJ, Sleigh JW: An electroencephalogram metric of temporal complexity tracks psychometric impairment caused by low-dose nitrous oxide. Anesthesiology 2021; 134:202–18
14. Schartner M, Seth A, Noirhomme Q, Boly M, Bruno MA, Laureys S, Barrett A: Complexity of multi-dimensional spontaneous EEG decreases during propofol induced general anaesthesia. PLoS One 2015; 10:e0133532
15. Sarasso S, Boly M, Napolitani M, Gosseries O, Charland-Verville V, Casarotto S, Rosanova M, Casali AG, Brichant JF, Boveroux P, Rex S, Tononi G, Laureys S, Massimini M: Consciousness and complexity during unresponsiveness induced by propofol, xenon, and ketamine. Curr Biol 2015; 25:3099–105
16. Pal D, Li D, Dean JG, Brito MA, Liu T, Fryzel AM, Hudetz AG, Mashour GA: Level of consciousness is dissociable from electroencephalographic measures of cortical connectivity, slow oscillations, and complexity. J Neurosci 2020; 40:605–18
17. Bai Y, Liang Z, Li X, Voss LJ, Sleigh JW: Permutation Lempel–Ziv complexity measure of electroencephalogram in GABAergic anaesthetics. Physiol Meas 2015; 36:2483–501

18. Lempel A, Ziv J: Complexity of finite sequences. IEEE Trans Inf Theory 1976; 22: 75–81
19. Fernández A, Quintero J, Hornero R, Zuluaga P, Navas M, Gómez C, Escudero J, García-Campos N, Biederman J, Ortiz T: Complexity analysis of spontaneous brain activity in attention-deficit/hyperactivity disorder: Diagnostic implications. Biol Psychiatry 2009; 65:571–7
20. Fernández A, Zuluaga P, Abásolo D, Gómez C, Serra A, Méndez MA, Hornero R: Brain oscillatory complexity across the life span. Clin Neurophysiol 2012; 123:2154–62
21. Casali AG, Gosseries O, Rosanova M, Boly M, Sarasso S, Casali KR, Casarotto S, Bruno MA, Laureys S, Tononi G, Massimini M: A theoretically based index of consciousness independent of sensory processing and behavior. Sci Transl Med 2013; 5:198ra105
22. Eagleman SL, Vaughn DA, Drover DR, Drover CM, Cohen MS, Ouellette NT, MacIver MB: Do complexity measures of frontal EEG distinguish loss of consciousness in geriatric patients under anesthesia? Front Neurosci 2018; 12:645
23. Li D, Mashour GA: Cortical dynamics during psychedelic and anesthetized states induced by ketamine. Neuroimage 2019; 196:32–40
24. von Elm E, Altman DG, Egger M, Pocock SJ, Gøtzsche PC, Vandenbroucke JP; STROBE Initiative: The Strengthening the Reporting of Observational Studies in Epidemiology (STROBE) statement: Guidelines for reporting observational studies. J Clin Epidemiol 2008; 61:344–9
25. Delorme A, Makeig S: EEGLAB: An open source toolbox for analysis of single-trial EEG dynamics including independent component analysis. J Neurosci Methods 2004; 134:9–21
26. Malviya S, Voepel-Lewis T, Tait AR, Merkel S, Tremper K, Naughton N: Depth of sedation in children undergoing computed tomography: Validity and reliability of the University of Michigan Sedation Scale (UMSS). Br J Anaesth 2002; 88:241–5
27. Vlisides PE, Li D, Zierau M, Lapointe AP, Ip KI, McKinney AM, Mashour GA: Dynamic cortical connectivity during general anesthesia in surgical patients. Anesthesiology 2019; 130:885–97
28. Mitra P, Bokil H: Observed Brain Dynamics. Oxford, Oxford University Press, 2008
29. Deco G, Cabral J, Saenger VM, Boly M, Tagliazucchi E, Laufs H, Van Someren E, Jobst B, Stevner A, Kringelbach ML: Perturbation of whole-brain dynamics *in silico* reveals mechanistic differences between brain states. Neuroimage 2018; 169:46–56
30. Kim H, Moon JY, Mashour GA, Lee U: Mechanisms of hysteresis in human brain networks during transitions of consciousness and unconsciousness: Theoretical principles and empirical evidence. PLoS Comput Biol 2018; 14:e1006424
31. Moon JY, Lee U, Blain-Moraes S, Mashour GA: General relationship of global topology, local dynamics, and directionality in large-scale brain networks. PLoS Comput Biol 2015; 11:e1004225
32. Kim M, Lee U: Alpha oscillation, criticality, and responsiveness in complex brain networks. Netw Neurosci 2020; 4:155–73
33. van den Heuvel MP, Sporns O: Rich-club organization of the human connectome. J Neurosci 2011; 31:15775–86
34. Hagmann P, Sporns O, Madan N, Cammoun L, Pienaar R, Wedeen VJ, Meuli R, Thiran J-P, Grant PE: White matter maturation reshapes structural connectivity in the late developing human brain. Proc Natl Acad Sci USA 2010: 107:19067–72
35. Kim M, Kim S, Mashour GA, Lee U: Relationship of topology, multiscale phase synchronization, and state transitions in human brain networks. Front Comput Neurosci 2017; 11:55
36. Caminiti R, Carducci F, Piervincenzi C, Battaglia-Mayer A, Confalone G, Visco-Comandini F, Pantano P, Innocenti GM: Diameter, length, speed, and conduction delay of callosal axons in macaque monkeys and humans: Comparing data from histology and magnetic resonance imaging diffusion tractography. J Neurosci 2013; 33:14501–11
37. Whitford TJ, Rennie CJ, Grieve SM, Clark CR, Gordon E, Williams LM: Brain maturation in adolescence: Concurrent changes in neuroanatomy and neurophysiology. Hum Brain Mapp 2007; 28:228–37
38. Uddin LQ, Supekar KS, Ryali S, Menon V: Dynamic reconfiguration of structural and functional connectivity across core neurocognitive brain networks with development. J Neurosci 2011; 31:18578–89
39. Anokhin AP, Birbaumer N, Lutzenberger W, Nikolaev A, Vogel F: Age increases brain complexity. Electroencephalogr Clin Neurophysiol 1996; 99:63–8
40. McCarthy MM, Brown EN, Kopell N: Potential network mechanisms mediating electroencephalographic beta rhythm changes during propofol-induced paradoxical excitation. J Neurosci 2008; 28:13488–504
41. Baker MR, Baker SN: The effect of diazepam on motor cortical oscillations and corticomuscular coherence studied in man. J Physiol 2003; 546:931–42
42. Buchsbaum MS, Hazlett E, Sicotte N, Stein M, Wu J, Zetin M: Topographic EEG changes with benzodiazepine administration in generalized anxiety disorder. Biol Psychiatry 1985; 20:832–42
43. Mashour GA, Roelfsema P, Changeux JP, Dehaene S: Conscious processing and the global neuronal workspace hypothesis. Neuron 2020; 105:776–98

44. Tononi G, Boly M, Massimini M, Koch C: Integrated information theory: From consciousness to its physical substrate. Nat Rev Neurosci 2016; 17:450–61
45. Hudetz AG, Liu X, Pillay S, Boly M, Tononi G: Propofol anesthesia reduces Lempel–Ziv complexity of spontaneous brain activity in rats. Neurosci Lett 2016; 628:132–5
46. Blain-Moraes S, Tarnal V, Vanini G, Bel-Behar T, Janke E, Picton P, Golmirzaie G, Palanca BJA, Avidan MS, Kelz MB, Mashour GA: Network efficiency and posterior alpha patterns are markers of recovery from general anesthesia: A high-density electroencephalography study in healthy volunteers. Front Hum Neurosci 2017; 11:328
47. Shortal BP, Hickman LB, Mak-McCully RA, Wang W, Brennan C, Ung H, Litt B, Tarnal V, Janke E, Picton P, Blain-Moraes S, Maybrier HR, Muench MR, Lin N, Avidan MS, Mashour GA, McKinstry-Wu AR, Kelz MB, Palanca BJ, Proekt A; ReCCognition Study Group: Duration of EEG suppression does not predict recovery time or degree of cognitive impairment after general anaesthesia in human volunteers. Br J Anaesth 2019; 123:206–18
48. Segalowitz SJ, Santesso DL, Jetha MK: Electrophysiological changes during adolescence: A review. Brain Cogn 2010; 72:86–100
49. Purdon PL, Pierce ET, Mukamel EA, Prerau MJ, Walsh JL, Wong KF, Salazar-Gomez AF, Harrell PG, Sampson AL, Cimenser A, Ching S, Kopell NJ, Tavares-Stoeckel C, Habeeb K, Merhar R, Brown EN: Electroencephalogram signatures of loss and recovery of consciousness from propofol. Proc Natl Acad Sci USA 2013; 110:E1142–51
50. Davidson AJ, Sale SM, Wong C, McKeever S, Sheppard S, Chan Z, Williams C: The electroencephalograph during anesthesia and emergence in infants and children. Paediatr Anaesth 2008; 18:60–70

ANESTHESIOLOGY REFLECTIONS FROM THE WOOD LIBRARY-MUSEUM

After the Ether Dome, Bulfinch Drafted His Way to the U.S. Capitol

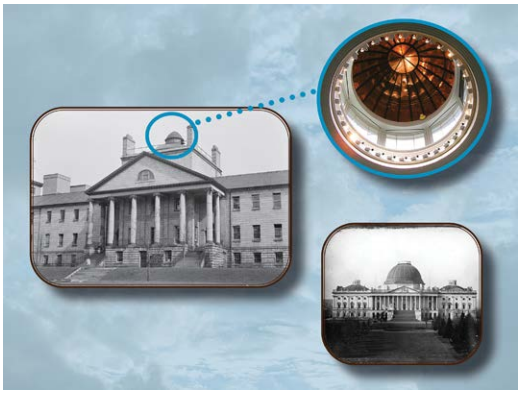

Boston's Ether Dome (*encircled, left*), the crown of Massachusetts General Hospital's Bulfinch Building (*left*), soared to fame 175 years ago after William T. G. Morton's public demonstration of ether anesthesia. Designated a National Historic Landmark in 1965, the Ether Dome is more than a captivating copper cupola. Blending essential function with elegant form, the design featured windows (*upper right*) to illuminate the surgical theater below. Its draftsman was Charles Bulfinch, a Bostonian architect renowned for his neoclassical style. A year into construction of his namesake building, Bulfinch was recruited to be the "Architect of the Capitol" in Washington, D.C. His design for the United States Capitol Dome (*lower right*), in contrast to that of the Ether Dome, relied more on form than function. Its imposing size and aesthetic symbolized the strength of the young republic, while its problematic wooden construction required frequent repairs. Although diminutive in its dimensions, the Ether Dome would prove to be Bulfinch's more enduring legacy; his original Capitol Dome was replaced with a larger cast-iron version in 1863. (Copyright © the American Society of Anesthesiologists' Wood Library-Museum of Anesthesiology.)

Melissa L. Coleman, M.D., Penn State College of Medicine, Hershey, Pennsylvania, and Jane S. Moon, M.D., University of California, Los Angeles, California.